

# PROCEEDINGS OF SPIE

[SPIEDigitallibrary.org/conference-proceedings-of-spie](https://www.spiedigitallibrary.org/conference-proceedings-of-spie)

## Large-scale 2D Surface-Micromachined Optical Ultrasound Transducer (SMOUT) array for 3D computed tomography

Zhiyu Yan, Jun Zou

Zhiyu Yan, Jun Zou, "Large-scale 2D Surface-Micromachined Optical Ultrasound Transducer (SMOUT) array for 3D computed tomography," Proc. SPIE 12379, Photons Plus Ultrasound: Imaging and Sensing 2023, 123790K (9 March 2023); doi: 10.1117/12.2649277

**SPIE.**

Event: SPIE BiOS, 2023, San Francisco, California, United States

# Large-scale 2D surface-micromachined optical ultrasound transducer (SMOUT) array for 3D acoustic tomography

Zhiyu Yan\*, Jun Zou

Department of Electrical and Computer Engineering, Texas A&M University, College Station, TX, 77843, USA

## ABSTRACT

This paper reports a new 2D surface-micromachined optical ultrasound transducer (SMOUT) array consisting of  $350 \times 350$  elements with highly uniform optical and acoustic performances. Each SMOUT element consists of a vacuum-sealed Fabry-Perot (F-P) interferometric cavity formed by two parallel partially reflective distributed Bragg reflectors (DBRs). Optical mapping in the  $4 \text{ cm} \times 4 \text{ cm}$  center region of the SMOUT array shows that the optical resonance wavelength (ORW) of more than 94% of the elements falls within a narrow range smaller than 10 nm. The center frequency, acoustic bandwidth, and noise equivalent pressure (NEP) of the elements are determined to be 3.5 MHz, 5 MHz, and 20.7 Pa (with 16 times of signal averaging) over a bandwidth of 10 MHz, respectively. The stability testing of the SMOUT elements shows little variation in their ORW under large ambient temperature fluctuation and during continuous water immersion. To demonstrate its imaging capability, 2D and 3D PACT based on the SMOUT array is conducted with no interrogation wavelength tuning. These results show that the SMOUT array could overcome some of the major limitations in existing 2D ultrasound transducer arrays and provide a promising solution for achieving high-speed 3D acoustic imaging.

**Keywords:** Surface micromachining; optical ultrasound transducer (OUT); photoacoustic (PA); ultrasound; computed tomography (CT)

## 1. INTRODUCTION

High-sensitivity and high-density 2D ultrasound transducer arrays are critical for high-performance 3D acoustic imaging, including pulse-echo ultrasound [1] and photoacoustic tomography [2]. Currently, the most commonly used transducer arrays are either piezoelectric [3] or capacitive [4], which convert the ultrasound signals into electrical charges or capacitance change. Because the amount of charge generation or capacitance change is surface-area dependent, the sensitivity of both piezoelectric and capacitive transducer elements will become poor when the transducer element has to be made small, especially in the case of high-density 2D arrays. In addition, they require electrical interface to read out the signals, which makes the fabrication and operation of large 2D transducer arrays extremely complex and costly. In contrast, optical ultrasound transducers (OUTs) function based on ultrasound-modulated light transmission or reflection [5-7], their output signal is mainly determined by the ultrasound pressure level and the intensity of the interrogation light. Therefore, they can achieve high sensitivity even with a small transducer element size. What's more, the ultrasound signals can be read out "wirelessly" via different optical means. These two unique features make OUTs ideal candidates for making high-sensitivity and high-density 2D transducer arrays. However, one fundamental challenge in OUTs is that their optical and acoustic properties are highly sensitive to the variations in materials and fabrication conditions, and therefore could scatter in a wide range. Without good uniformity, reading out the ultrasound data from an OUT array will require continual tuning of the (optical) operation parameters [8], which is a tedious and slow process and therefore seriously limits the imaging speed.

To address this issue, we report a new 2D surface-micromachined optical ultrasound transducer (SMOUT) array based on Fabry-Perot interferometry. With an optimized surface micromachining process [9], highly uniform SMOUT elements are created on the entire wafer. Experiments are conducted to characterize both the optical and acoustic performances and stability of the SMOUT array. To demonstrate its imaging capability, both 2D and 3D photoacoustic computed tomography (PACT) experiments are also conducted. Results show that the SMOUT array has excellent optical and acoustic uniformity, high acoustic sensitivity, broad acoustic bandwidth and good stability, which is suitable for parallel data acquisition to enable high-speed 3D acoustic tomography.

## 2. SENSOR DESIGN AND FABRICATION

As shown in Fig. 1(a), a SMOUT element consists of a vacuum F-P cavity formed by two parallel distributed Bragg reflectors (DBRs). Impinging ultrasound waves vibrate the top flexible DBR diaphragm and tune the F-P cavity length. As a result, the optical resonance wavelength (ORW) (i.e., the wavelength where the reflectivity reaches its minimum, defined as  $\lambda_0$  in Fig. 1(b)) will be shifted, which modulates the optical reflectance of the SMOUT element at the wavelength near  $\lambda_0$ . To maximize the linear range, the SMOUT elements are interrogated at a wavelength that is located around the middle point ( $\lambda_{bias}$ ) between the ORW and the wavelength giving highest reflectivity. Each DBR consists of multiple silicon oxide and nitride pairs, whose thicknesses are adjusted to provide an optical length (the product of thickness and refractive index) equal to one quarter of the DBR's center wavelength. The top diaphragm has a diameter of 70  $\mu\text{m}$  and an overall thickness of  $\sim 3 \mu\text{m}$ . Its flexural-mode response in water is simulated with COMSOL Multiphysics, which shows a resonance frequency of 4.3 MHz. To widen the bandwidth, a Parylene film ( $\sim 10 \mu\text{m}$ ) is coated onto the top diaphragm to increase the damping effect. The element pitch is 140  $\mu\text{m}$ , which is smaller than half of the acoustic wavelength of  $\sim 350 \mu\text{m}$  at a frequency of 4.3 MHz in water. This helps to eliminate the grating lobes in directivity profile and aliasing in spatial sampling. The entire SMOUT array consists of  $350 \times 350$  elements within a square area of  $5 \times 5 \text{ cm}^2$  (Fig. 1(c)).

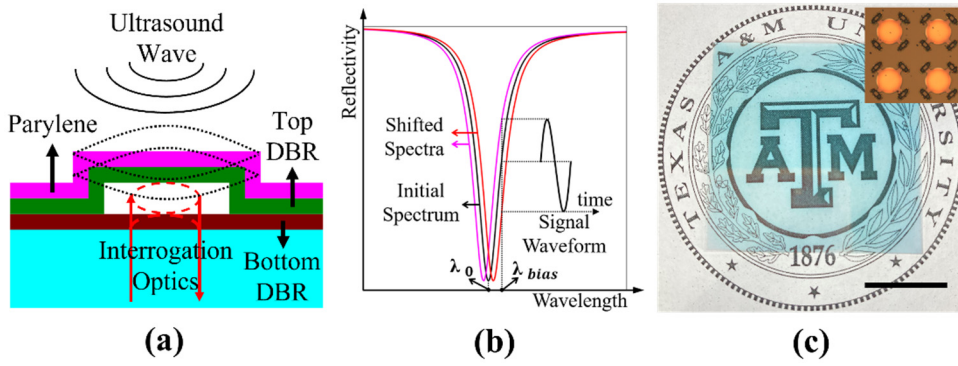


Fig. 1. (a) Schematic showing the cross-section and ultrasound detection mechanism of a SMOUT element. (b) Schematic showing the modulation of reflectivity at interrogation wavelength  $\lambda_{bias}$  by acoustic-induced reflection spectrum shift. (c) Top view showing the entire SMOUT array (the scale bar is 2 cm; the subfigure shows  $2 \times 2$  SMOUT elements).

## 3. TESTING AND CHARACTERIZATION

### 3.1 Optical resonance wavelength (ORW)

The ORW of each SMOUT element determines its optical readout condition and needs to be made as uniform as possible. An optical setup is built to characterize the ORW of the SMOUT elements in the array (Fig. 2) [10]. The light sources consist of a 765–815 nm CW tunable laser for the characterization and a halogen lamp for illuminating the measured SMOUT element. The laser and the collimated white light beams are combined and focused onto the center region of a SMOUT element. Reflected light from the SMOUT element is coupled into a single mode (SM) fiber coupler and received by a photo detector. The output of the photodetector is amplified and recorded by the data acquisition card (DAQ), which is synchronized by the trigger signal from the tunable laser. The recorded time-domain signal during one sweeping cycle of the tunable laser is converted into the reflection spectrum. Fig. 3 (a) shows a representative reflection spectrum of the SMOUT elements, which indicates a typical ORW of 805 nm. To characterize the ORW uniformity, the SMOUT array is scanned with a step of 0.98 mm  $\times$  0.98 mm (every 7 elements) and a total range of 40  $\times$  40 steps ( $\sim 4 \text{ cm} \times 4 \text{ cm}$ ). Fig. 3(b) shows a mapped image of the distribution of the ORW. 94% of the elements (except those at the corners) have an ORW within a narrow range of 802–812 nm.

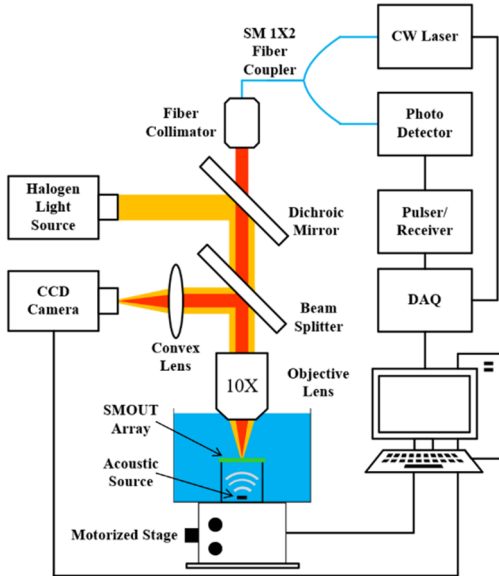


Fig. 2. Experimental setup for optical and acoustic characterization of the SMOUT array.

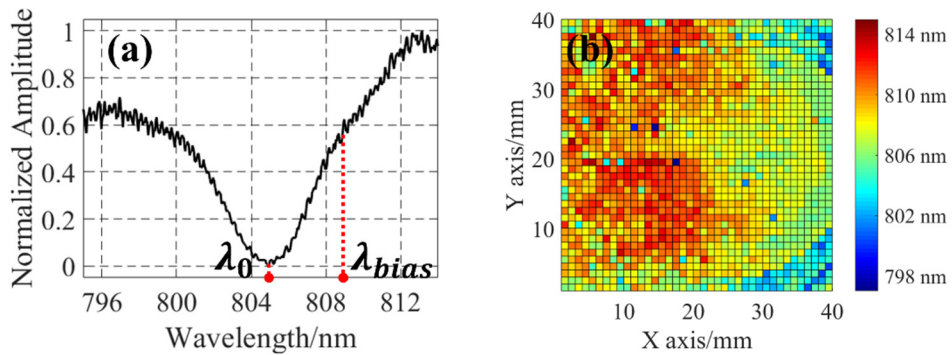


Fig. 3. (a) Representative optical reflection spectrum of the SMOUT elements. (b) ORW mapping in the  $40 \text{ mm} \times 40 \text{ mm}$  center region of the SMOUT array.

### 3.2 Acoustic response

Driven by acoustic pressure, the top diaphragm of the SMOUT element vibrates in flexural mode. The coating of a viscoelastic polymeric (Parylene) layer helps to enhance the damping to the diaphragm vibration and broaden the acoustic bandwidth. PA testing with a wide-band black-tape target is conducted to characterize the acoustic response of the SMOUT elements. Figs. 4(a) and 4(b) show the received PA signal (by a SMOUT element) and its acoustic frequency spectrum after FFT (Fast Fourier Transformation), respectively. The center frequency and the 6-dB bandwidth are around 3.5 MHz and 5 MHz, respectively, indicating a wide acoustic bandwidth of 140%.

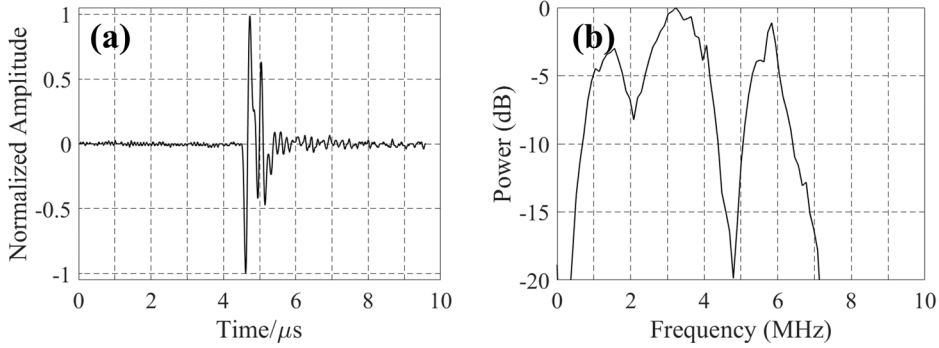


Fig. 4. (a) Representative PA signal received from the black tape target and (b) its acoustic frequency spectrum after FFT.

### 3.3 Noise equivalent pressure (NEP)

The overall sensitivity of an SMOUT element together with the optical read-out setup is evaluated by the noise equivalent pressure (NEP). NEP is defined as the detected acoustic pressure level when the signal to noise ratio (SNR) reaches unity in the low-frequency limit (when acoustic wavelength is much larger than F-P cavity length), which can be calculated as  $NEP = P/SNR$ , where  $P$  is the acoustic pressure (Pa) received by the sensor. The SMOUT array is used to detect ultrasound waves from a lead zirconate titanate (PZT) plate (with 5-MHz center frequency). Acoustic pressure generated by the PZT plate is also measured by a needle hydrophone, which is estimated to be 30.2 kPa. Twenty-five elements within the 4 cm  $\times$  4 cm center region of the SMOUT array are measured, and the averaged signal amplitude is 7.3 V. The peak-to-peak noise amplitude (mainly from the CW laser, photo detector and the amplifier) is 5.0 mV with 16 signal averaging. The averaged NEP is calculated as 20.7 Pa over a bandwidth of 10 MHz. The NEP of the 25 elements ranges between 19.5 Pa and 22.5 Pa (Fig. 5), which means that the sensitivity of the elements is quite uniform across the entire SMOUT array.

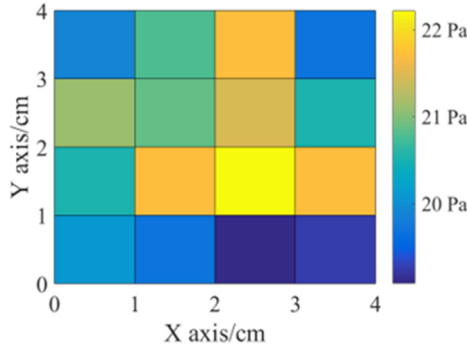


Fig. 5. NEP distribution at 25 locations in the 4 cm  $\times$  4 cm center region of the SMOUT array.

### 3.4 Temperature and temporal stability

For acoustic imaging, long-time water immersion of the transducer array is required for acoustic coupling. Also, the ambient temperature could fluctuate with different operation parameters. Therefore, ORW drift of the SMOUT elements due to water immersion and ambient temperature change could be a potential issue. To evaluate the stability of the SMOUT elements, two sets of testing are conducted. Firstly, the ORWs of three SMOUT elements are acquired under an ambient temperature ranging from 25°C to 55°C with a step of 5°C. The mean values of the ORW vs. the ambient temperature is shown in Fig. 6(a). The standard deviation (STD) of the ORW is 0.18 nm, which is only 0.02% of the mean value (Relative STD). Secondly, the ORWs of three SMOUT elements immersed in water under room temperature are continuously monitored for one week. The mean values of the ORWs in each day are plotted in Fig. 6(b), which show a STD of 0.33 nm and a relative STD of 0.04%. The small shifts in ORW indicate the excellent temperature and temporal stability of the SMOUT elements.

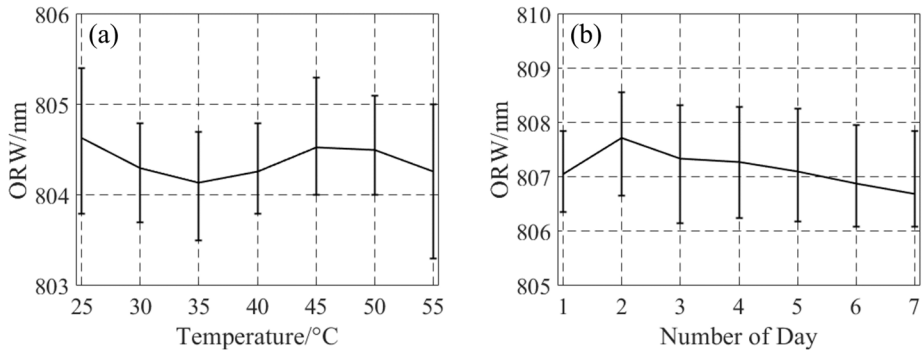


Fig. 6. Average value of ORWs of three tested SMOUT elements (a) at different ambient temperature and (b) immersed in water for seven consecutive days. Error bars are included in both plots to show the deviation of the ORW.

#### 4. IMAGING EXPERIMENT

To demonstrate the imaging capability of the SMOUT array, PACT experiments are conducted to evaluate the field of view (FOV), imaging depth, and contrast-to-noise ratio (CNR). The interrogation wavelength is set to 808 nm for the entire imaging process without tuning. The imaging targets consist of three dot-shape pencil leads (1mm long, 0.5mm in diameter) fixed sparsely below the SMOUT array. The SMOUT array is located at x-y plane ( $z = 0$ ), and the three targets are located 20 mm, 25 mm, and 30 mm below the SMOUT array, respectively (Figs. 7(a) and (b)). Two PA imaging experiments are conducted: 2D B-mode imaging with one pencil lead (Target #2 illustrated in Fig. 7(b)) and 3D volumetric imaging with the three pencil leads as the target. For the 2D B-mode imaging, the interrogation laser beam acquires the PA signals from a 1D array of SMOUT elements (along the y axis) right above the target with the scanning range and interval of 3 cm and 140  $\mu$ m (every element), respectively. Fig. 7(c) shows the reconstructed B-mode image which has a high CNR of 66.4 dB. For the 3D volumetric imaging, signals from the center region of the SMOUT array (3 cm  $\times$  3 cm) are obtained and used for imaging reconstruction. Fig. 7(d) shows the reconstructed PA image of the three targets, which shows a high CNR of 60.6 dB.

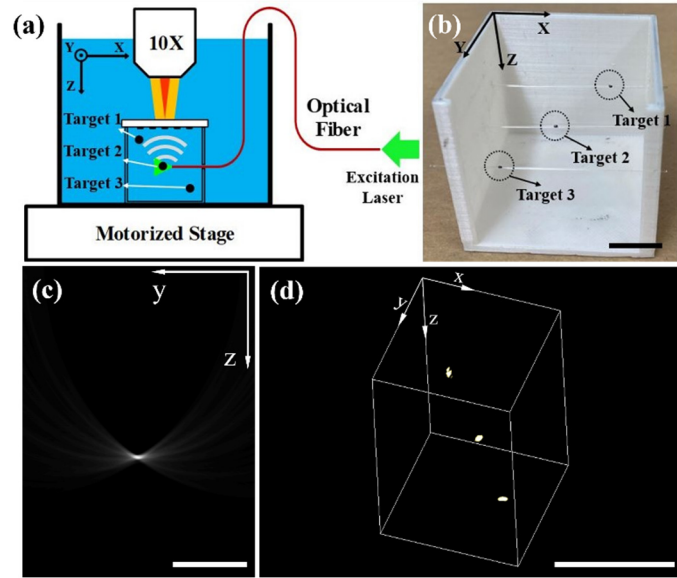


Fig. 7. (a) Experimental setup for PACT imaging test. (b) Three pencil lead targets (scalebar 10mm). (c) 2D B-scan PA image of one pencil lead (scalebar 10 mm). (d) 3D volumetric PA image of three pencil leads (scalebar 20 mm).

## 5. CONCLUSION

In conclusion, a new large-scale 2D SMOUT array has been designed, fabricated, and characterized. The experimental results show that the SMOUT array can have high element density, excellent uniformity, superior acoustic sensitivity, and good temperature and temporal stability. As a result, it requires no interrogation condition adjustment or tuning for different elements, which drastically improves the data acquisition speed. In addition, it can be made optically transparent over a wide range of optical wavelengths to facilitate the delivery of laser pulses for PA excitation. These features make the SMOUT array a promising solution for high-speed 3D acoustic imaging applications.

## ACKNOWLEDGMENTS

This work was supported in part by National Science Foundation (CMMI-1852184, NRI-1925037 and CBET-2036134).

## REFERENCES

- [1] Thomas L. Szabo, Diagnostic Ultrasound Imaging: Inside Out, 2nd ed., Waltham, MA: Academic Press, 2014.
- [2] Lihong V. Wang, Photoacoustic Imaging And Spectroscopy, Boca Raton, FL: CRC Press, 2009.
- [3] L. Lin, P. Hu, X. Tong, S. Na, R. Cao, X. Yuan, D. C. Garrett, J. Shi, K. Maslov and L. V. Wang, "High-speed three-dimensional photoacoustic computed tomography for preclinic research and clinical translation," *Nat. Commun.*, vol. 12, no. 1, Feb. 2021, Art. no. 882.
- [4] S. Vaithilingam, T.-J. Ma, Y. Furukawa, I. O. Wygant, X. Zhuang, A. De La Zerda, Omer Oralkan, Aya Kamaya, Sanjiv s. Gambhir, R. Brooke Jeffrey, and B. T. Khuri-yakub, "Three-dimensional photoacoustic imaging using a two-dimensional CMUT array," *IEEE T. Ultrason. Ferr.*, vol. 56, no. 11, pp. 2411-2419, Feb. 2009.
- [5] P. C. Beard, F. Perennes, and T. N. Mills, "Transduction Mechanisms of the Fabry-Perot Polymer Film Sensing Concept for Wideband Ultrasound Detection," *IEEE T. Ultrason. Ferr.*, vol. 46, no. 6, pp. 1575-1582, Feb. 1999.
- [6] Z. Shao, Q. Rong, F. Chen and X. Qiao, "High-spatial-resolution ultrasonic sensor using a micro suspended-core fiber," *Opt. Express*, vol. 26, no. 8, pp. 10820-10832, Apr. 2018.
- [7] Z. Shao, Y. Wu, Z. Sun, W. Wang, Z. Liu, C. Zhang, J. Bi, and E. Song, "Excellent repeatability, all-sapphire Fabry Perot optical Pressure sensor based on wet etching and direct bonding for Harsh Environment Application," *Opt. Express*, vol. 29, no. 13, pp. 19831-19838, June 2021.
- [8] P. C. Beard, "Two-Dimensional Ultrasound Receive Array Using an Angle-Tunned Fabry-Perot Polymer Film Sensor for Transducer Field Characterization and Transmission Ultrasound Imaging," *IEEE T. Ultrason. Ferr.*, vol. 52, no. 6, pp. 1002-1012, June 2005.
- [9] J. M. Bustillo, R. T. Howe, and R. S. Muller, "Surface micromachining for microelectromechanical systems," in *Proc. IEEE*, Quebec City, Qc, CA, Aug. 1998, pp. 1552-1574.
- [10] Z. Yan and J. Zou, "Large-scale surface-micromachined optical ultrasound transducer (SMOUT) array for photoacoustic computed tomography," *Opt. Express*, vol. 30, no. 11, pp. 19069-19080, May 2022.